Icariin promotes the repair of bone marrow mesenchymal stem cells in rabbit knee cartilage defects via the BMP/Smad pathway

Feng Jiao[1], Wang Tang[2], Jie Wang[2], Donghua Liu[2], Hongyi Zhang[1], Dongming Tang[1]

[1]Department of Joint Surgery, Guangzhou Hospital of Integrated Traditional and Western Medicine, Guangzhou, China; [2]Department of Spinal Surgery, Guangzhou Hospital of Integrated Traditional and Western Medicine, Guangzhou, China

Contributions: (I) Conception and design: F Jiao; (II) Administrative support: F Jiao, W Tang; (III) Provision of study materials or patients: H Zhang, D Tang; (IV) Collection and assembly of data: F Jiao, J Wang; (V) Data analysis and interpretation: F Jiao, D Liu; (VI) Manuscript writing: All authors; (VII) Final approval of manuscript: All authors.

Correspondence to: Feng Jiao. Chief Physician, Master Tutor, Department of Joint Surgery, Guangzhou Hospital of Integrated Traditional and Western Medicine, 87 Yingbin Road, Huadu District, Guangzhou, China. Email: twjiaofeng123@163.com.

Background: Icariin (ICA) has been widely used in the treatment of osteoporosis. However, the potential mechanism of its critical role in repairing knee cartilage damage still needs to be further clarified.

Methods: First, rabbit bone marrow mesenchymal stem cells (BMSCs) were isolated, cultured, and identified. Subsequently, BMSCs were treated with different concentrations of ICA. Cell Counting Kit 8 (CCK-8) and 5-ethynyl-2'-deoxyuridine (EdU) were used to evaluate the cell proliferation in each group. Alcian Blue staining, immunofluorescence, and western blotting were used to evaluate the ability of BMSCs to differentiate cartilage. In addition, a rabbit knee cartilage injury model was established. Evaluation of cartilage defects in each group was performed according to the classification system outlined by the International Cartilage Repair Society (ICRS). Hematoxylin and eosin (HE), Alcian Blue, and immunohistochemistry were used to analyze the pathological status of knee cartilage.

Results: *In vitro*, the results showed that ICA promoted the cartilage differentiation of BMSCs as well as cell proliferation. In addition, ICA promoted the expression of type II collagen (*COL2A1*), aggrecan, and bone morphogenetic protein 2 (*BMP2*) in BMSCs, while BMP-Smad inhibitor (Noggin) reversed the repair effect of ICA on BMSCs. *In vivo*, our results showed that the ICRS score of the BMSC and ICA treatment group was higher. Moreover, BMSC and ICA treatment promoted the proliferation of chondrocytes and repaired the cartilage-like tissue on the surface of cartilage defect.

Conclusions: The combined application of ICA and BMSCs can repair rabbit knee cartilage injury by regulating the BMP/Smads pathway, indicating that ICA and BMSCs may be a viable clinical treatment strategy for knee cartilage damage.

Keywords: Icariin (ICA); bone marrow mesenchymal stem cell (BMSC); knee cartilage damage; BMP/Smads

Submitted Apr 19, 2022. Accepted for publication Jun 08, 2022.
doi: 10.21037/atm-22-2515
View this article at: https://dx.doi.org/10.21037/atm-22-2515

Introduction

Osteoarthritis (OA), an affliction with a large social burden, is defined as a degenerative joint disease involving cartilage and its surrounding tissues (1). In the early stages of OA, the surface of the articular cartilage changes little. With further changes in the composition and structure of articular cartilage, cartilage integrity is destroyed, chondrocytes undergo apoptosis, and OA ultimately arises thereby (2). In the treatment of OA, improving cartilage damage and enhancing cartilage protection are considered to be promising avenues of development, with the promotion of cartilage regeneration thus also being seen as a propitious line of OA treatment research (3). Mesenchymal stem cells (MSCs) can be easily grown in culture, have the ability to

differentiate into cartilage, and thus are an alternative cell source for cartilage repair (4,5) and are of considerable significance for the regeneration of cartilage.

Icariin (ICA) is the main bioactive ingredient extracted from the Chinese herbal medicine *Epimedium brevicornum Maxim*, which has been shown to reduce cartilage degradation (6). A clinical trial has reported that ICA was effective in preventing postmenopausal osteoporosis with relatively low side effects (7). ICA has been extensively studied as a potential small molecular drug for bone regeneration, and its desirable properties are generally thought to arise from the estrogen-like effects it exerts on osteoblasts as a result of the structural similarity between ICA and β-estradiol (8,9). ICA not only promotes chondrogenic differentiation (10) and osteoblastogenesis, but also inhibits osteoclastogenesis (11), leading to bone formation. ICA has been shown to promote osteogenic differentiation by regulating the osteoclastogenesis inhibitory factor (*OPG*) to Receptor Activator of Nuclear Factor-κB Ligand (*RANKL*) expression ratio (12). Furthermore, Wang *et al.* (13) reported that ICA could increase alkaline phosphatase (ALP) activity and upregulate the messenger RNA (mRNA) expression levels of *Runx2*, *ALP*, *COL I*, and *OCN*. Song *et al.* (8) reported that ICA promoted MC3T3-E1 cell differentiation through activation of the extracellular regulated protein kinases (ERK) and c-Jun N-terminal kinase (JNK) signaling pathways. Finally, ICA has been shown to inhibit cartilage tissue destruction (14). Therefore, ICA may play an important role in protecting against cartilage damage and promoting cartilage repair.

The bone morphogenetic protein 2 (*BMP2*) signaling pathway is a critical regulator of cartilage and bone formation (15,16). In addition, BMP2 binds to its receptors to induce phosphorylation of drosophila mothers against decapentaplegic protein(Smad) 1/5/9 (15) and then regulates the early stage of osteoblast differentiation through transcription factors, such as *Id1*, *Dlx5*, and *Runx* (17,18). Studies in developmental biology have revealed that transcription factors, including *Runx2* and *β-catenin*, play a key role in the regulation of bone marrow MSC (BMSC) differentiation (19,20). Moreover, *Runx2* expression is upregulated by *BMP2*-activated Smad proteins, and also interacts with Smad proteins to induce osteoblast differentiation (21,22).

There are many factors affecting the proliferation and differentiation of BMSC, such as inflammation, mechanical stress (23), and some specific cytokines. Inflammation was considered as an inhibitory role in the cartilage regeneration (24). Studies suggest that ICA can regulate BMP and Runx signaling and enhance osteoblastogenesis *in vitro* (25,26). Although evidence suggests that ICA can attenuate hypoxia-induced apoptosis in osteoblasts (27), it is uncertain whether ICA acts on BMP2/Smad signaling pathways. Therefore, the aim of the present study was to investigate the therapeutic effect of ICA in repairing knee cartilage damage, and for the first time, we explore the regulation of ICA on BMP2/Smad signal pathway in BMSC osteogenic induction. We present the following article in accordance with the ARRIVE reporting checklist (available at https://atm.amegroups.com/article/view/10.21037/atm-22-2515/rc).

Methods

Cell isolation and culture

New Zealand rabbits (1 month old) were purchased from the Experimental Animal Center of Southern Medical University. Rabbit BMSCs were isolated from rabbit bone marrow. Cells were cultured in Dulbecco's Modified Eagle Medium (DMEM; Hyclone, South Logan, UT, USA) containing 100 U/mL penicillin/streptomycin and 10% fetal bovine serum (FBS; Hyclone). The medium was changed every 3 days. Experiments were performed under a project license granted by institutional committee board of Guangzhou Hospital of Integrated Traditional and Western Medicine (No. E-20210427), in compliance with national guidelines for the care and use of animals. A protocol was prepared before the study without registration.

Determination of surface antigens of BMSCs

Third-generation BMSCs grown to 80–90% were collected, digested with 0.25% trypsin at room temperature and centrifuged, and the cell pellet was collected. The pellet was washed with phosphate-buffered saline (PBS) and made into a 1×10^5/mL cell suspension. Following this, 10 μL each of fluorescently labeled phenotypic antibodies, CD29, CD44, CD90, CD34, and CD45, was added to 100 μL of the cell suspension. Surface antigen expression was detected using flow cytometry (BD-FACSVerse, San Jose, CA, USA).

BMSC osteogenic induction and Alizarin Red staining

Osteogenic induction medium (each 100 mL) containing

10% FBS (Gibco, Grand Island, NY, USA), 2% double antibody, 0.01 μmol/L dexamethasone (Solarbio, Beijing, China), 10 mmol/L β-sodium glycerophosphate (Solarbio), and 50 mg/L ascorbic acid (Solarbio) was prepared. Cells were cultured with osteogenic induction medium and stained with Alizarin Red. The residual medium was washed off with sterile PBS, and the cells were fixed with 4% paraformaldehyde for 15 min. The residual fixative was washed with double-distilled water, and 2 mL of 0.2% Alizarin Red staining solution (Solarbio) was added to each well for a staining duration of 30 min. After the residual dye was washed off, the staining results were observed microscopically.

Chondrogenic induction of BMSCs and Alcian Blue staining

Cartilage induction medium containing 10% FBS, 1% double antibody, 100 nM dexamethasone, 50 μg/mL Vc, 100 μg/mL sodium pyruvate, 40 ug/mL proline, 50 mg/mL insulin transferrin selenite, and 10 ng/mL tumor growth factor beta (TGF- β) was prepared. The cells were cultured in osteogenic induction medium and stained with Alcian Blue. The cells were then fixed with 4% paraformaldehyde for 15 min, and the residual stationary solution was washed away with PBS. The cells were then soaked with Alcian acidification solution (Solarbio) for 3 min and dyed with Alcian staining solution (Solarbio) for 30 min. After the residual dyes were washed off, the dyeing results were observed microscopically.

Adipogenesis induction of BMSCs and Oil Red O staining

Lipid induction medium containing 10% FBS, 1% double antibody, 10 μg/mL insulin (Solarbio), 1 μM dexamethasone (Solarbio), 0.5 mM IBMX (Solarbio), and 0.1 mM indomethacin (Solarbio) was prepared. The cells were cultured in adipogenic induction medium and stained with Oil Red O. The cells were fixed with 10% neutral formaldehyde for 30 min, and the residual fixative was washed off with PBS. Next, 0.5% Oil Red O working solution was added to the cells, which were dyed in dark for 1 h. The residual dye was washed off with isopropanol, and the dyeing results were observed microscopically.

Cell viability assay

Cell viability was determined with Cell Counting Kit 8 (CCK-8; Dojindo, Kumamoto, Japan). Cells were seeded into 96-well plates at a density of 2×10^3 cells/well, and cells were treated with different concentrations of ICA (0, 0.1, 1, and 10 μM). Cell viability was determined at specific times using the CCK-8 kit (and absorbance at 450 nm was measured.

Cell proliferation analysis

BeyoClick EdU-555 cell proliferation detection kit (Beyotime, Shanghai, China) was used to determine the proliferation ability of BMSCs. Proliferated BMSCs were incubated with EdU working solution (10 μM) for 3 h at 37 ℃. The incubated BMSCs were washed with PBS to remove residual liquid and fixed with 4% paraformaldehyde for 15 min. Cells were incubated with 0.3% Triton-X100 (Merck Millipore, Billerica, MA, USA) for 15 min at room temperature and stained with reaction solution (C0075S, Beyotime). The staining results were observed using a fluorescence microscope (Olympus, Tokyo, Japan).

Immunofluorescence

Treated cells were fixed with 4% paraformaldehyde for 30 min at room temperature. Cells were permeabilized with 0.1% Triton X-100 and blocked with 1% bovine serum albumin. Cells were incubated with rabbit polyclonal anti-COL2A1, BMP2 and Runx2 antibodies (Abcam, Cambridge, UK) overnight at 4 ℃. Cells were incubated with CM-Dil-labeled goat anti-rabbit secondary antibody (Boster, Wuhan, China) at room temperature and stained with DAPI. Cells were observed by fluorescence microscopy (Olympus).

Real-time quantitative reverse transcription polymerase chain reaction

Total cellular RNA was extracted using Trizol reagent (Takara Bio Inc., Shiga, Japan). Reverse transcription was performed using the Bestar^{TM} qPCR RT Kit (cat. No. 2220, DBI (Bioscience, Shanghai, China) according to the manufacturer's instructions. Real-time analysis was performed on a Stratagene real-time polymerase chain reaction (PCR) instrument (Agilent, Santa Clara, CA, USA) using the BestarTM qPCR MasterMix Kit (cat. No. 2043, DBI). The relative expression levels of each gene were quantified using the $2^{-\Delta\Delta Ct}$ method. The primer sequences are shown in *Table 1*.

Table 1 The sequences of primers

ID	Sequence (5'-3')
GAPDH.F	CCTCGTCTCATAGACAAGATGGT
GAPDH.R	GGGTAGAGTCATACTGGAACATG
Aggrecan.F	GGAGCTTTGGACTTTGGCGGA
Aggrecan.R	ACGTGCAGTGGTGGCTGTGAC
Sox9.F	CCCACCTCTCTTACCTCTCTC
Sox9.R	ATCCAGTCTCTCTTCCACTCC
COL2A1.F	CCTTGGTGGAAACTTTGCTGC
COL2A1.R	TGCCTTGAAATCCTTGCGGTC
MMP-13.F	TTCTACCACACAAACCACACT
MMP-13.R	CTTCCTCGGACAAATCATCAT
Runx2.F	CTCCGAAATGCCTCTGCTGTTATGA
Runx2.R	CGGGGTCCATCCACTGTAACTTTAA
Smad1.F	AATCAGCAGAGGAGATGTTCA
Smad1.R	AAGCGGTTCTTATTGTTGGAC
BMP2.F	ATCCAGTCTCTCTTCCACTCC
BMP2.R	GGTGATCAGCCAGGGGAAAGG

Western blot

BMSCs cells were collected and lysed with RIPA cell lysate. The protein content in the samples was detected using a bicinchoninic acid (BCA) protein assay kit (Beyotime). Protein samples were electrophoresed on 12% SDS-PAGE, and protein bands were transferred to polyvinylidene fluoride (PVDF) membranes (Millipore, Billerica, MA, USA). Membranes were blocked with 5% nonfat milk for 2 h at room temperature, incubated with primary antibodies overnight at 4 ℃, and then incubated with horseradish peroxidase (HRP)–conjugated secondary antibodies for 2 h at room temperature. Protein bands were visualized by chemiluminescence using an enhanced chemiluminescence (ECL) kit (Thermo Fisher Scientific, Waltham, MA, USA).

Construction of rabbit knee cartilage injury model

Female New Zealand rabbits (weight 2.5 kg) were purchased from the Experimental Animal Center of Southern Medical University and raised in an environment with a temperature of 22 ℃ and a relative humidity of 55%. Rabbits were anesthetized intravenously with 3% sodium pentobarbital (40 mg/kg). An incision was made at the medial edge of the patellar ligament of the right knee, and a hole with a diameter of 3 mm and a depth of 4 mm was drilled. The depth was a full-thickness cartilage defect with bleeding red bone marrow. The patella was reset, the wound was sutured, and 800,000 units of penicillin were injected into the gluteal muscle every day for 3 days after operation.

Animal grouping and treatment

All animal models were randomly divided into 5 groups with 7 animals in each group. They were divided into sham operation (sham), operation (operation), operation + BMSCs, operation + ICA, and operation + BMSCs + ICA groups. The specific treatment process was performed as follows: on the third day after modeling, the animals in sham group received an incision on the skin tissue, were injected with normal saline (1 mL), and were then sutured without cartilage damage; the animals in the operation group were injected with an equal volume of normal saline (1 mL) into the joint cavity; the animals in the BMSC group were injected with 1 mL of rabbit BMSC (1×10^7 cells) into the joint cavity; the animals in the ICA group were injected with 1 mL of 10 μM ICA into the ear vein; and the animals in the BMSCs + ICA group were treated with an injection into the joint cavity of 1 mL of rabbit BMSC (1×10^7 cells) preincubated with 10 μM ICA for 72 h. The used concentration of ICA was adjusted based on a previous report (28). The administration frequency of each group of animals was once a week, with a total of 3 doses. After 8 weeks of observation, the rabbits were euthanized and the knee joints were removed. Cartilage damage was assessed based on the International Cartilage Repair Society (ICRS) gross morphology assessment scale for cartilage repair (*Table 2*).

Hematoxylin and eosin (HE) staining and Toluidine Blue staining

The lower end of the obtained femur was fixed with paraformaldehyde for at least 24 h and then soaked in 10% EDTA for 3 weeks. Tissues were dehydrated, embedded with paraffin wax, and cut into 5-μm thick sections. Sections were deparaffinized and dehydrated sequentially with xylene and graded alcohol, stained with hematoxylin staining solution for 5 min, washed with water for 10 min, treated with 1% hydrochloric acid ethanol for 5 s, washed with water again for 1 min, stained again with 0.5% eosin for 5 min, and finally treated once more with graded alcohol and xylene. The slides were sealed with neutral gum, and

Table 2 Baroscopic evaluation of cartilage repair according to ICRS

Feature	Score
Degree of defect repair	
In level with surrounding cartilage	4
75% repair of defect depth	3
50% repair of defect depth	2
25% repair of defect depth	1
0% repair of defect depth	0
Integration to border zone	
Complete integration with surrounding cartilage	4
Demarcating border <1 mm	3
3/4 of graft integrated, 1/4 with a notable border >1 mm width	2
1/2 of graft integrated with surrounding cartilage, 1/2 with a notable border >1 mm	1
From no contact to 1/4 of graft integrated with surrounding cartilage	0
Macroscopic appearance	
Intact smooth surface	4
Fibrillated surface	3
Small, scattered fissures or cracks	2
Several, small, or few but large fissures	1
Total degeneration of grafted area	0
Overall repair assessment	
Grade I: normal	12
Grade II: nearly normal	8-11
Grade III: abnormal	4-7
Grade IV: severely abnormal	1-3

ICRS, international society for cartilage repair.

the results were observed under a microscope after air-drying. The pretreatment of Toluidine Blue staining was the same as that of HE staining. Deparaffinized sections were stained with 1% Toluidine Blue for 3 min and treated with graded alcohol and xylene. The staining results were observed under a light microscope.

Immunohistochemistry

The sections were deparaffinized and dehydrated in xylene and graded alcohol, and antigen retrieval was performed with antigen retrieval solution. The sections were incubated overnight at 4 ℃ with rabbit anti-BMP2, Runx2, and Smad1 antibodies, respectively. Next, the sections were incubated with HRP-conjugated goat anti-rabbit secondary antibody for 1 h min at room temperature. The sections were stained with DAB staining solution and counterstained with hematoxylin. The staining results were observed under a light microscope.

Statistical analysis

Data were analyzed using GraphPad Prism 8.0.2 software (GraphPad Software, Inc., San Diego, CA, USA). All experiments were repeated 3 times independently, and the experimental results are expressed as mean ± standard

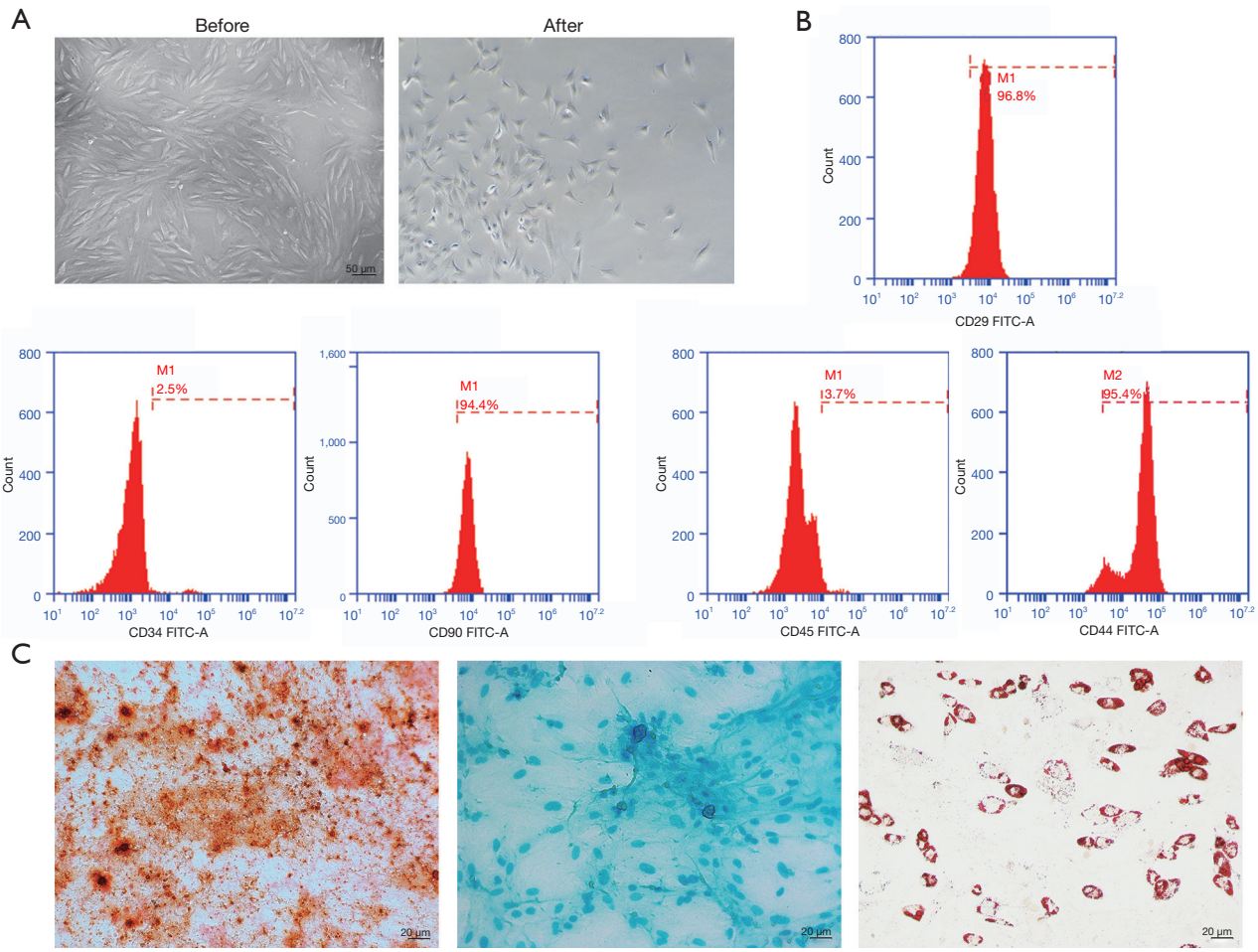

Figure 1 Characterization and differentiation potential of BMSCs. (A) Morphological observation of BMSCs before and after induction. (B) The expression levels of marker molecules CD29, CD34, CD90, CD45, and CD44 of BMSCs were determined by flow cytometry. (C) Alizarin Red S, Alcian Blue, and Oil Red O staining were used to detect the osteogenic, chondrogenic, and adipogenic differentiation levels of BMSCs, respectively. BMSC, bone marrow mesenchymal stem cell.

deviation. Differences between 2 groups were analyzed by Student's *t*-test, and comparisons between multiple groups were performed using 1-way analysis of variance (ANOVA) and Tukey's post hoc test. A P value <0.05 was considered to indicate a statistically significant difference.

Results

Characterization and differentiation potential of BMSCs

The third-generation BMSCs were a homogeneous population with a spindle shape, and cytomorphological observations showed that BMSCs isolated from bone marrow also possessed this feature. The morphology of the induced BMSCs was significantly changed. The cells become rounded and grew tentacles, mostly triangular in shape (*Figure 1A*). Flow cytometry results showed that the cells were positive for the typical BMSCs markers CD29 (96.8%), CD44 (95.4%), and CD90 (94.4%), while being negative for CD34 (2.5%) and CD45 (3.7%; *Figure 1B*). BMSCs have the potential to differentiate into osteoblasts, chondrocytes, and adipocytes. Alizarin Red S, Alcian Blue, and Oil Red O staining showed that BMSCs cultured under osteogenic differentiation conditions formed mineralized nodules, exhibited increased proteoglycan expression, and generated lipid droplets, respectively (*Figure 1C*).

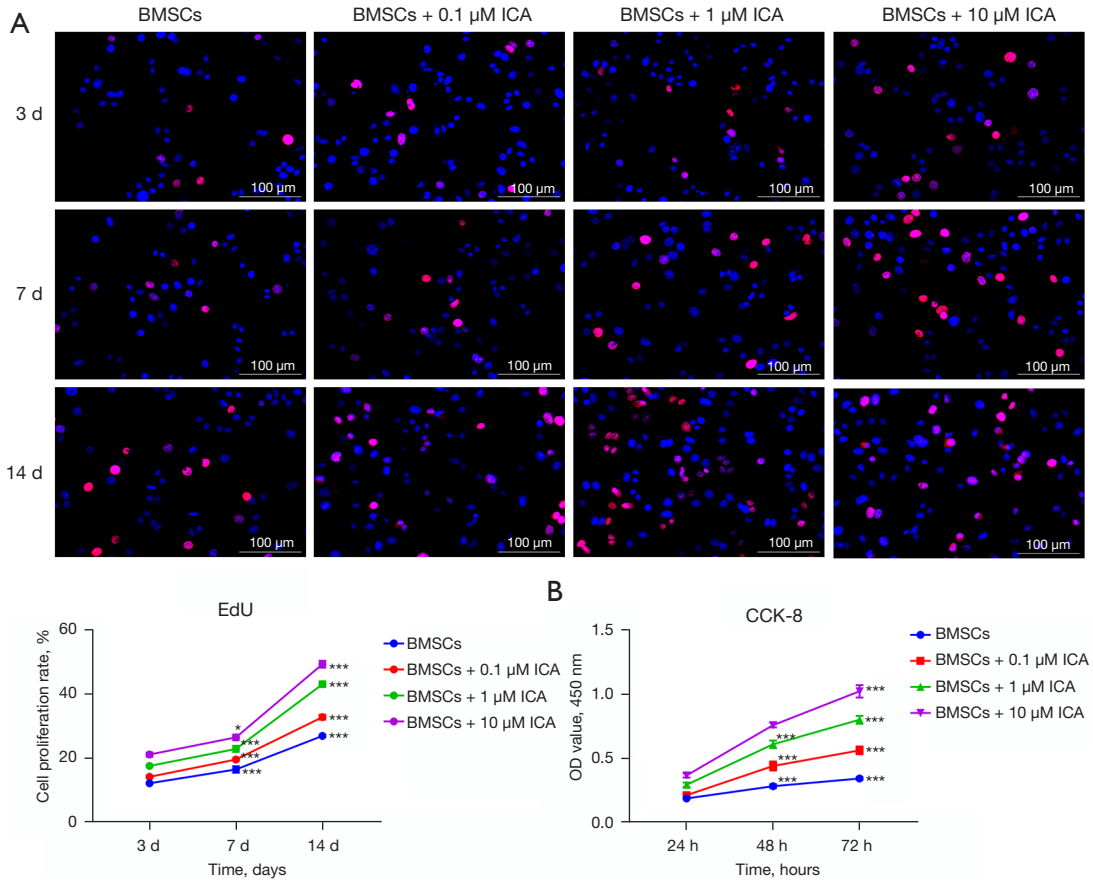

Figure 2 ICA promoted BMSCs proliferation. (A) An EdU proliferation assay was used to determine the cell proliferation level of BMSCs treated with different concentrations of ICA (0, 0.1, 1, and 10 μM) at different durations (3, 7, and 14 d). (B) The cell viability of BMSCs treated with different concentrations of ICA (0, 0.1, 1, and 10 μM) at different durations (24, 48, and 72 h) was determined by CCK8 assay. *, P<0.05; ***, P<0.001 compared with the BMSCs group. ICA, icariin; BMSC, bone marrow mesenchymal stem cell.

This indicated that the isolated BMSCs had the ability to differentiate into osteogenic, chondrogenic, and adipogenic types.

ICA promoted the proliferation of BMSCs

In this study, different concentrations of ICA were used to act on cells, and the EdU proliferation experiments showed that ICA treatment significantly increased the red fluorescence area in a concentration-dependent manner and promoted the proliferation of BMSCs (*Figure 2A*). In addition, ICA increased cell viability in a time-dependent and concentration-dependent manner (*Figure 2B*).

ICA induced chondrogenic differentiation of BMSCs

Cells were treated with 0.1, 1, or 10 μM of ICA, and the ability of cells to differentiate into chondroblasts was tested on days 3, 7, and 14. Alcian Blue staining showed that BMSCs expressed more polysaccharide glycans with increasing incubation time and ICA concentration (*Figure 3*). The subsequent experiments further confirmed the ability of ICA to induce chondrogenic differentiation of BMSCs. The immunofluorescence results of COL2A1 showed that ICA treatment significantly increased the expression level of COL2A1 compared with the BMSC group in a time- and concentration-dependent manner

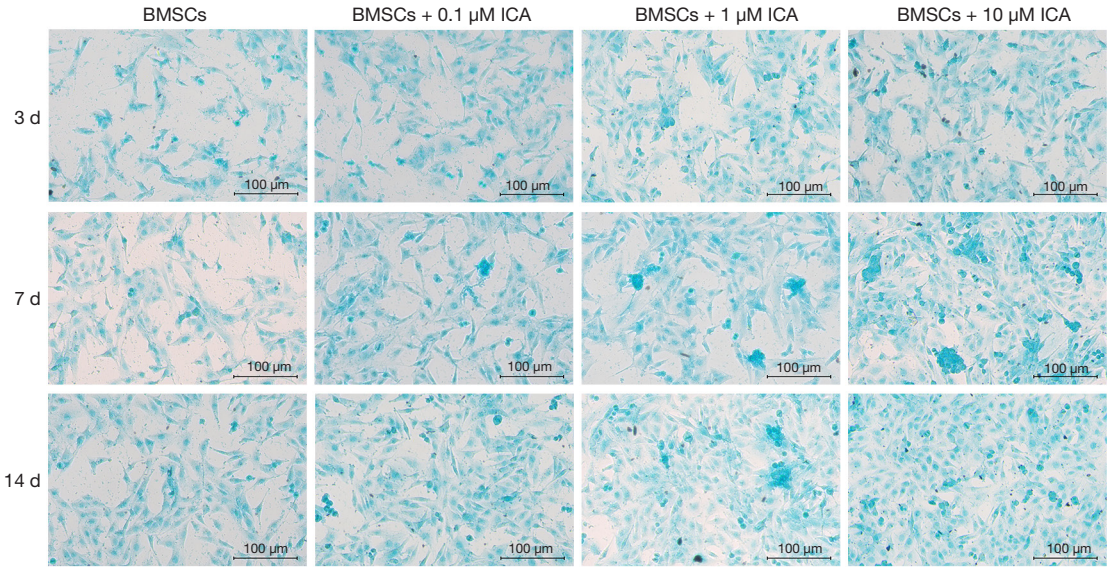

Figure 3 ICA induced chondrogenic differentiation of BMSCs. Alcian Blue staining was used to determine the ability of BMSCs to differentiate into chondrogenic cells. BMSCs were treated with different concentrations of ICA (0, 0.1, 1, and 10 μM) and the levels of polysaccharide glycans (blue area) were detected at different times (3, 7, and 14 d). ICA, icariin; BMSC, bone marrow mesenchymal stem cell.

(*Figure 4*). Reverse-transcription PCR results showed that ICA treatment upregulated the mRNA expression levels of *Aggrecan*, *COL2A1*, *BMP2*, *Runx2*, *Smad1*, *MMP-13*, and *Sox9* (*Figure 5A*). Western blot results further confirmed that ICA induced a gradual increase in the expression levels of these chondrogenesis-related proteins in a time- and concentration-dependent manner (*Figure 5B*).

ICA induced chondrogenic differentiation of BMSCs by upregulating the level of BMP2

To confirm whether ICA induces chondrogenic differentiation of BMSCs through the regulation of BMP2, we treated cells with an inhibitor of BMP2 protein (Noggin). This revealed that ICA significantly increased the protein expression levels of Runx2, COL2A1, Aggrecan, matrix metalloproteinase 13 (MMP-13), p-Smad1, and Smad1 in BMSCs. The protein levels when cells were cotreated with ICA and Noggin were significantly lower than those treated with ICA alone (*Figure 6A*). Immunization results for BMP2 and Runx2 also showed that Noggin treatment reduced the high levels of BMP2 and Runx2 induced by 1 μM of ICA (*Figure 6B*). Alcian Blue staining results further demonstrated that Noggin treatment reduced the expression level of polysaccharide glycans induced by 1 μM of ICA (*Figure 6C*). The above results indicated that inhibiting the expression of *BMP2* and *Runx2* can reduce the chondrogenic differentiation of BMSCs induced by ICA, which induces the chondrogenic differentiation of BMSCs by upregulating the level of *BMP2* and *Runx2*.

Combination of ICA and BMSCs in the repair of knee cartilage injury in vivo

We subsequently assessed the repair level of damaged cartilage tissue after 8 weeks of BMSC and ICA treatment using the ICRS criteria. The mean ICRS score of the surgery group was much lower than that of the sham group, and the knee cartilage was severely damaged. ICRS scores were significantly increased after BMSC or ICA treatment. After the combined treatment of BMSCs and ICA, the ICRS score of the BMSC + ICA group increased significantly and was significantly higher than that of the BMSC alone and ICA alone groups (*Figure 6D*). The results of HE staining for the surgery group showed that the cartilage surface was irregular, the cartilage layer was narrowed, and the cartilage structure was severely damaged. After treatment with ICA or BMSCs alone, the damaged cartilage tissue was improved, and the combined use of ICA and BMSCs significantly restored the structure of the damaged cartilage tissue (*Figure 7*). The results of Toluidine Blue staining showed that compared with the operation

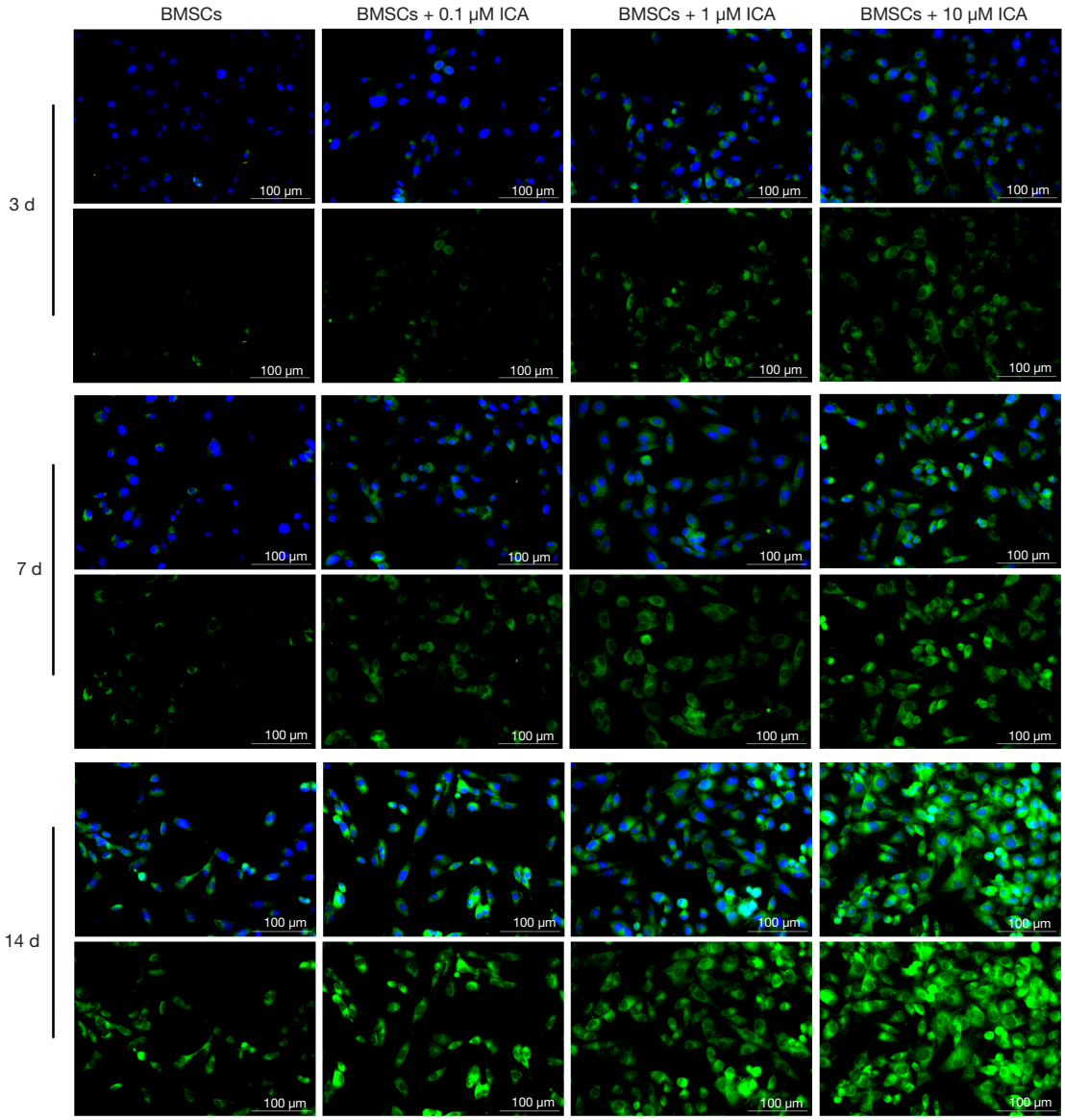

Figure 4 ICA induced chondrogenic differentiation of BMSCs. The expression levels of COL2A1 under different concentrations of ICA and different action times were determined by immunofluorescence. Blue is DAPI and green is the target protein. ICA, icariin; BMSC, bone marrow mesenchymal stem cell.

group, the ICA group, BMSC group and BMSC + ICA group had deeper Toluidine Blue staining, with the content of the extracellular matrix (ECM) being significantly upregulated in these groups (*Figure 7*). Furthermore, immunohistochemical results showed that ICA or BMSC treatment alone significantly increased the expression levels of BMP2, Runx2, and Smad1 in damaged cartilage tissue. Combination treatment with ICA and BMSC was more effective than treatment with ICA or BMSC alone (*Figure 8*).

Discussion

Due to its ability to stimulate estrogen receptor-dependent osteoblastic functions, ICA has multiple pharmacological properties with potency and protective effects (29-31). One *in vitro* experiment demonstrated that ICA can promote the proliferation and differentiation of osteoblasts and the DNA synthesis of BMCs (32). In addition, ICA has been shown alleviate mitochondrial dysfunction and decrease apoptosis

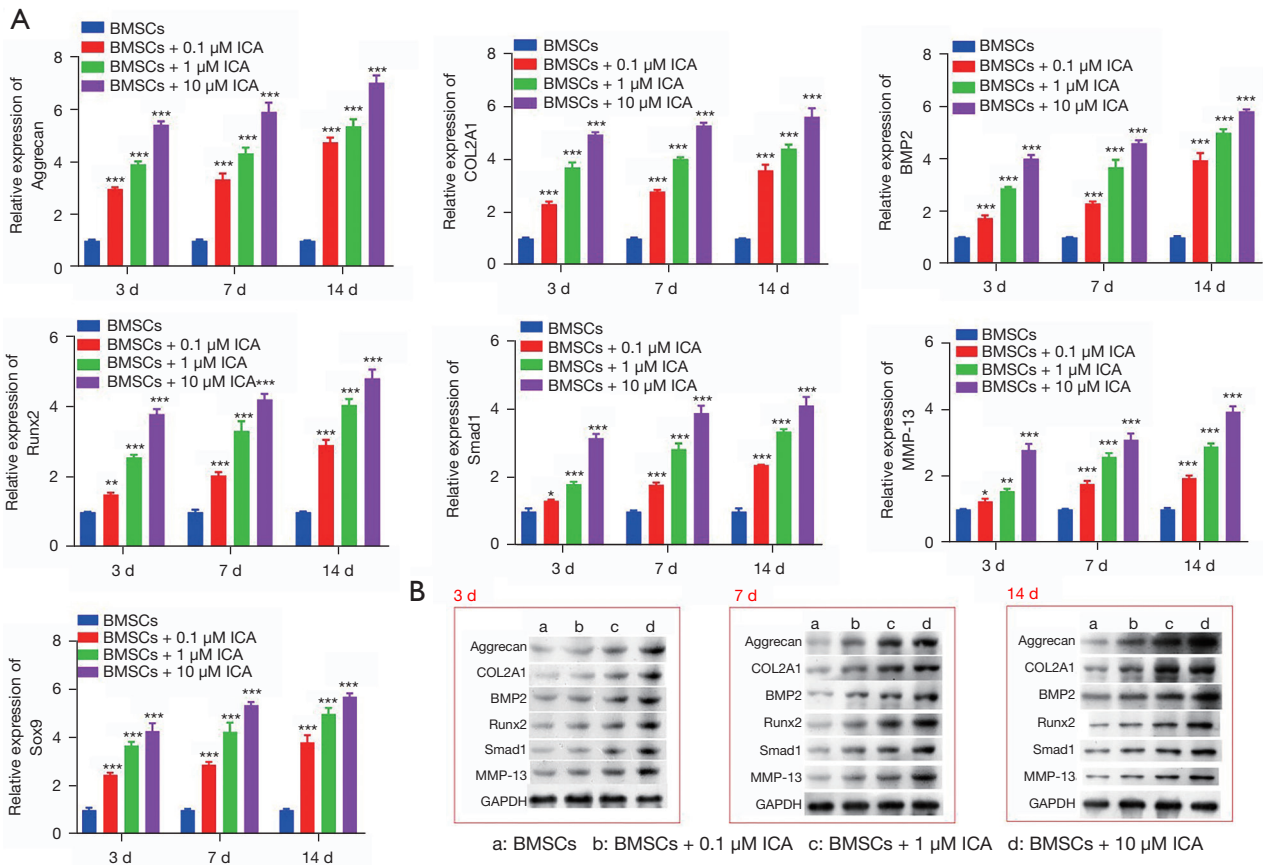

Figure 5 ICA promoted the expression of chondrogenesis-related genes. (A) ICA upregulated the mRNA expression levels of Aggrecan, COL2A1, BMP2, Runx2, Smad1, MMP-13, and Sox9. (B) ICA upregulated the protein expression levels of Aggrecan, COL2A1, BMP2, Runx2, Smad1, and MMP-13. *, P<0.05; **, P<0.01; ***, P<0.001 compared with the BMSCs group. ICA, icariin; BMSC, bone marrow mesenchymal stem cell.

in dilated cardiomyopathy (DCM) (33). Consistent with this, our study demonstrated that ICA exerts positive effects on cell proliferation as indicated by the increased cell proliferation and decreased cell apoptosis.

Articular cartilage is mainly composed of chondrocytes, ECM, and water (14), while bone marrow stromal cells retains the ability to differentiate into cartilage. Therefore, it is critically important to investigate the differentiation BMSCs as it pertains to the effects of ICA. To identify the role of ICA in cartilage repair, we established a cartilage injury model. Next, we histologically evaluated the width of cartilage injury and analyzed the pathological status of knee cartilage. Previous study reported that ICA could promote osteogenic differentiation by upregulating *BMAL1* expression through BMP signaling in BMSCs (25), while Shi *et al.* reported that ICA could induce osteogenic differentiation via activation of cAMP/PKA/CREB signaling pathway (30). In addition, ICA inhibits chondrocyte apoptosis and angiogenesis by regulating the TDP-43 signaling pathway (34). In the present study, we confirmed that ICA could effectively elevate the ability of BMSCs to differentiate cartilage. In addition to this, we discovered that ICA treatment led to a significant increase in the expression of hypertrophic cartilage markers (e.g., type X collagen and Aggrecan) during osteogenic differentiation. Of note, our findings showed that ICA treatment improved the articular cartilage injury through cell growth and differentiation.

Matrix metalloproteinases (MMPs) are multifunctional growth factors, which figure prominently in the development of inflammatory and immune diseases as well as in the damaging of cartilage and bone (35). BMP2 binds to the BMP receptor and then activates the cytoplasmic

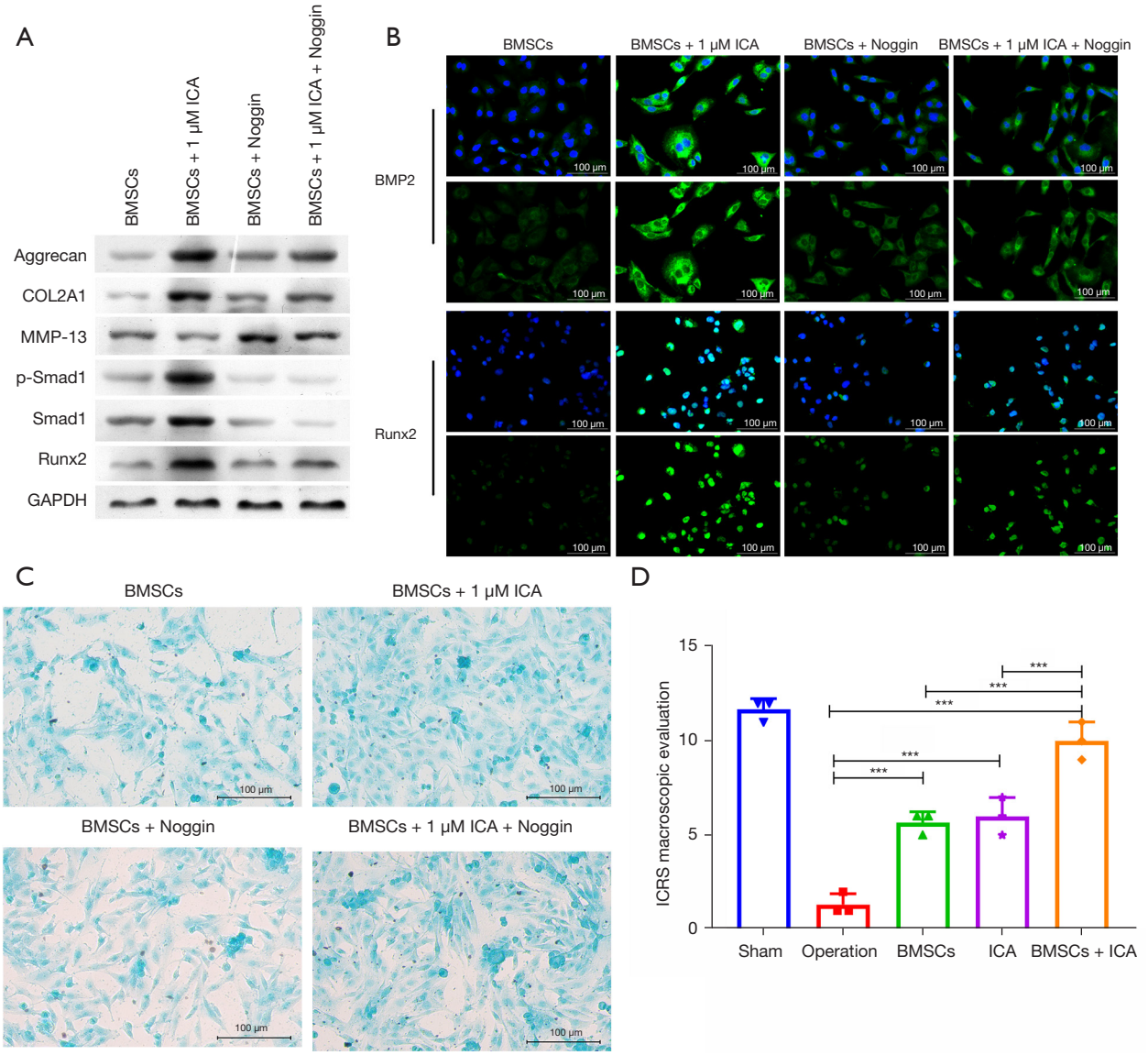

Figure 6 ICA induced the chondrogenic differentiation of BMSCs by regulating the level of BMP2. (A) The protein expression levels of Aggrecan, COL2A1, MMP-13, p-Smad1, Smad1, Runx2, and GAPDH in each group were detected by western blotting. Columns A, B, C, and D represent the BMSCs group, BMSCs + 1-μM ICA group, BMSCs + Noggin group, and BMSCs + 1-μM ICA + Noggin group, respectively. (B) The expression levels of BMP2 and Runx2 in cells of each group were determined by immunofluorescence. Blue is DAPI and green is the target protein. (C) The levels of polysaccharide glycans (blue area) in the cells of each group were determined by Alcian Blue staining. (D) Evaluation of the repair level of damaged cartilage tissue after BMSCs and/or ICA treatment according to ICRS criteria. ***, P<0.001 indicates statistical significance. ICA, icariin; BMSC, bone marrow mesenchymal stem cell; ICRS, international society for cartilage repair.

serine/threonine kinase of BMP receptor (BMPR)-I and Smad1/5/8, and this process was associated with cartilage damage. Phosphorylated Smad translocates into the nucleus and regulates the expression of target genes (36). Furthermore, *BMP2* has been shown to have an overall positive role in promoting bone regeneration (37). In this study, we verified the positive effects of ICA on the osteogenic differentiation of BMSCs. Likewise, Zhang *et al.*

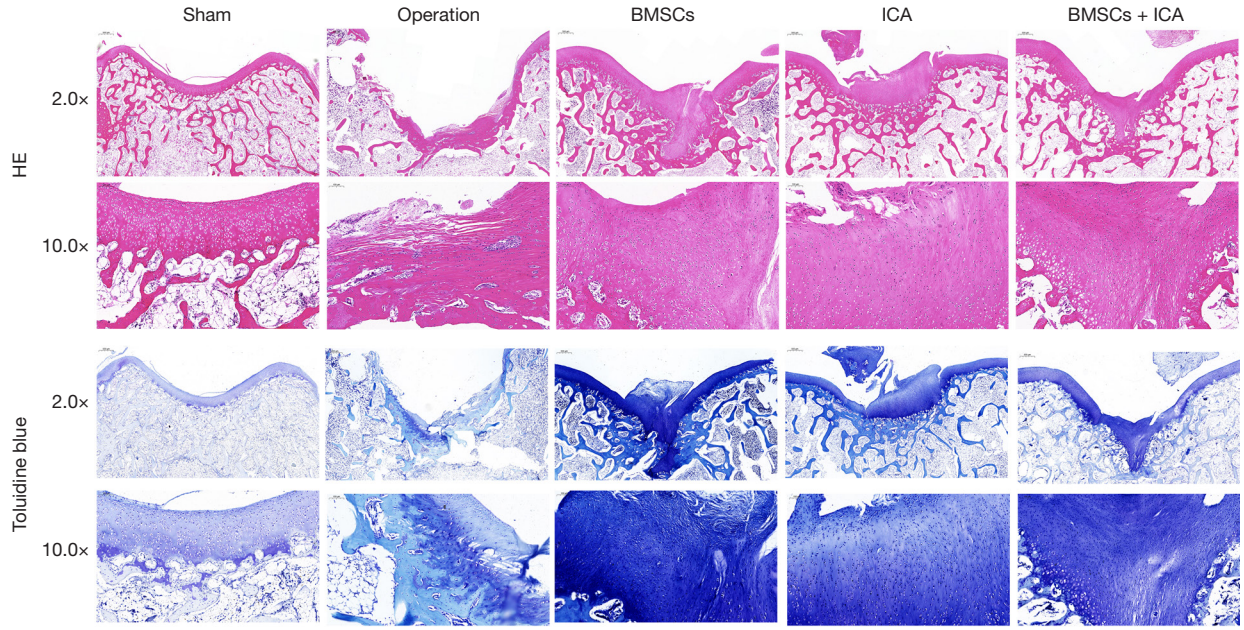

Figure 7 HE staining and toluidine blue staining results of each group. Seven rabbits in each group were used for surgical modeling, and after operation the rabbits was treated with injection of BMSCs or ICA. At the 8th week, bone and joints were preserved, and stained with hematoxylin and eosin and toluidine blue. ICA, icariin; BMSC, bone marrow mesenchymal stem cell.

found that ICA regulates *miR-23a-3p*–mediated osteogenic differentiation of BMSCs via BMP2/Smad5/Runx2 and WNT/β-catenin pathways (38). Moreover, in this study, the protein expression of BMP2 was significantly different between the ICA group and control group, indicating that *BMP2* might play an important role in the formation of ectopic ossification after muscle injury, a finding in line with that of another research (39). Consequently, it can be surmised that *BMP2* may also be vital to the process of BMSC differentiation. The goal of MSC-based therapy is to be able to promote engraftment and osteogenic differentiation of the transplanted cells. As an osteoinductive factor, *BMP2* is able to promote bone regeneration (39) and has widely used for bone regeneration as an osteoinductive adjuvant (40,41). However, BMP2 is a pleiotropic protein that can also exert adverse effects on the surrounding tissues, such as in the case of ectopic bone formation or the swelling of soft tissue (42,43). Therefore, the direct injection of BMSCs combined with ICA might be a good therapeutic candidate for cartilage repair. In the present study, the ICRS scores of the BMSC and ICA treatment group were higher than those of the other groups. Meanwhile, BMP-Smad inhibitor (Noggin) reversed the repair effect of ICA on BMSCs. This suggests that the BMP2-induced phosphorylation of Smad is essential for the proliferation of BMSCs. To the best of our knowledge, the present study provided evidence that the effect of ICA on BMSC was attenuated by Noggin. These results may provide a theoretical basis for using ICA in clinical treatment of neurobiological bone regeneration. In fact, there are a large number of Chinese herbal compounds that may be used to treat cartilage damage (44). Therefore, researchers need to make more efforts to study the specific mechanism of drugs promoting cartilage repair.

In conclusion, the present study showed that ICA could alter the expression of *COL2A1* and aggrecan, and induce the osteogenic differentiation of BMSC *in vitro*. Furthermore, it was shown that ICA could enhance the BMP2/Smad signaling pathway, indicating that the administration of ICA and BMSCs may be a viable clinical

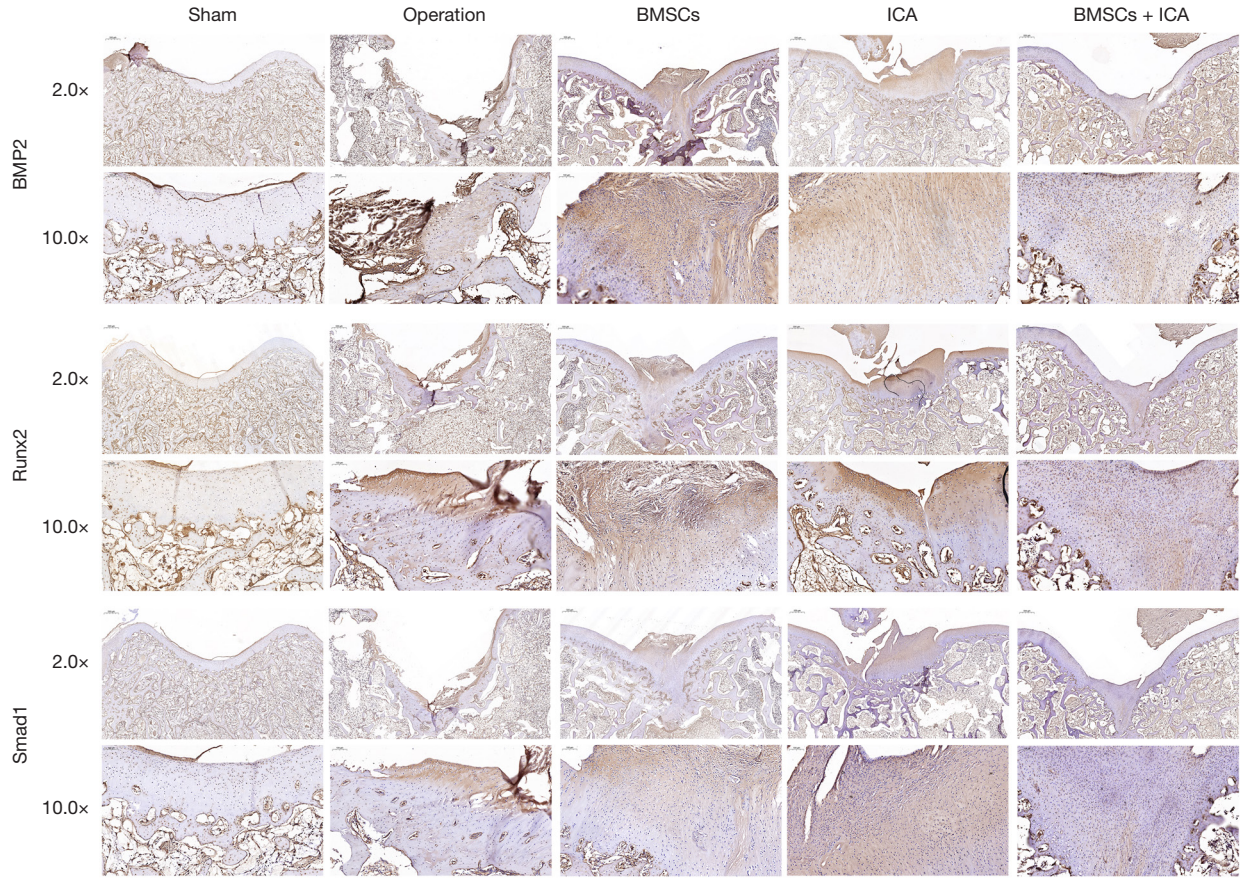

Figure 8 The immunohistochemical results of BMP2, Runx2, and Smad1 in each group. Seven rabbits in each group were used for surgical modeling, and after operation the rabbits was treated with injection of BMSCs or ICA. At the 8th week, expression of BMP2, Runx2, and Smad1 in bone and joints was detected by immunohistochemistry. ICA, icariin; BMSC, bone marrow mesenchymal stem cell.

treatment strategy for knee cartilage damage.

Acknowledgments

Funding: This study was supported by funding from the Natural Science Foundation of Guangdong Province (No. 2020A1515011085).

Footnote

Reporting Checklist: The authors have completed the ARRIVE reporting checklist. Available at https://atm.amegroups.com/article/view/10.21037/atm-22-2515/rc

Data Sharing Statement: Available at https://atm.amegroups.com/article/view/10.21037/atm-22-2515/dss

Conflicts of Interest: All authors have completed the ICMJE uniform disclosure form (available at https://atm.amegroups.com/article/view/10.21037/atm-22-2515/coif). All authors report that this study was supported by funding from the Natural Science Foundation of Guangdong Province (No. 2020A1515011085). The authors have no other conflicts of interest to declare.

Ethical Statement: The authors are accountable for all aspects of the work in ensuring that questions related to the accuracy or integrity of any part of the work are appropriately investigated and resolved. Experiments were performed under a project license granted by institutional committee board of Guangzhou Hospital of Integrated Traditional and Western Medicine (No. E-20210427), in compliance with national guidelines for the care and use of

animals.

References

1. Litwic A, Edwards MH, Dennison EM, et al. Epidemiology and burden of osteoarthritis. Br Med Bull 2013;105:185-99.
2. Xia B, Di Chen, Zhang J, et al. Osteoarthritis pathogenesis: a review of molecular mechanisms. Calcif Tissue Int 2014;95:495-505.
3. Li MH, Xiao R, Li JB, et al. Regenerative approaches for cartilage repair in the treatment of osteoarthritis. Osteoarthritis Cartilage 2017;25:1577-87.
4. De Bari C, Roelofs AJ. Stem cell-based therapeutic strategies for cartilage defects and osteoarthritis. Curr Opin Pharmacol 2018;40:74-80.
5. Meng HY, Lu V, Khan W. Adipose Tissue-Derived Mesenchymal Stem Cells as a Potential Restorative Treatment for Cartilage Defects: A PRISMA Review and Meta-Analysis. Pharmaceuticals (Basel) 2021;14:1280.
6. Luo Y, Zhang Y, Huang Y. Icariin Reduces Cartilage Degeneration in a Mouse Model of Osteoarthritis and is Associated with the Changes in Expression of Indian Hedgehog and Parathyroid Hormone-Related Protein. Med Sci Monit 2018;24:6695-706.
7. Wang Z, Wang D, Yang D, et al. The effect of icariin on bone metabolism and its potential clinical application. Osteoporos Int 2018;29:535-44.
8. Song L, Zhao J, Zhang X, et al. Icariin induces osteoblast proliferation, differentiation and mineralization through estrogen receptor-mediated ERK and JNK signal activation. Eur J Pharmacol 2013;714:15-22.
9. Rickard DJ, Monroe DG, Ruesink TJ, et al. Phytoestrogen genistein acts as an estrogen agonist on human osteoblastic cells through estrogen receptors alpha and beta. J Cell Biochem 2003;89:633-46.
10. Zhu Y, Ye L, Cai X, et al. Icariin-Loaded Hydrogel Regulates Bone Marrow Mesenchymal Stem Cell Chondrogenic Differentiation and Promotes Cartilage Repair in Osteoarthritis. Front Bioeng Biotechnol 2022;10:755260.
11. Ji R, Wu D, Liu Q. Icariin inhibits RANKL-induced osteoclastogenesis in RAW264.7 cells via inhibition of reactive oxygen species production by reducing the expression of NOX1 and NOX4. Biochem Biophys Res Commun 2022;600:6-13.
12. Wang F, Liu Z, Lin S, et al. Icariin enhances the healing of rapid palatal expansion induced root resorption in rats. Phytomedicine 2012;19:1035-41.
13. Wang Q, Cao L, Liu Y, et al. Evaluation of synergistic osteogenesis between icariin and BMP2 through a micro/meso hierarchical porous delivery system. Int J Nanomedicine 2017;12:7721-35.
14. Wei CC, Ping DQ, You FT, et al. Icariin Prevents Cartilage and Bone Degradation in Experimental Models of Arthritis. Mediators Inflamm 2016;2016:9529630.
15. Wu M, Chen G, Li YP. TGF-β and BMP signaling in osteoblast, skeletal development, and bone formation, homeostasis and disease. Bone Res 2016;4:16009.
16. Yang W, Guo D, Harris MA, et al. Bmp2 in osteoblasts of periosteum and trabecular bone links bone formation to vascularization and mesenchymal stem cells. J Cell Sci 2013;126:4085-98.
17. Ryoo HM, Lee MH, Kim YJ. Critical molecular switches involved in BMP-2-induced osteogenic differentiation of mesenchymal cells. Gene 2006;366:51-7.
18. Jang WG, Kim EJ, Lee KN, et al. AMP-activated protein kinase (AMPK) positively regulates osteoblast differentiation via induction of Dlx5-dependent Runx2 expression in MC3T3E1 cells. Biochem Biophys Res Commun 2011;404:1004-9.
19. Liu G, Vijayakumar S, Grumolato L, et al. Canonical Wnts function as potent regulators of osteogenesis by human mesenchymal stem cells. J Cell Biol 2009;185:67-75.
20. Ceccarelli G, Bloise N, Mantelli M, et al. A comparative analysis of the in vitro effects of pulsed electromagnetic field treatment on osteogenic differentiation of two different mesenchymal cell lineages. Biores Open Access 2013;2:283-94.
21. Mukherjee A, Rotwein P. Akt promotes BMP2-mediated osteoblast differentiation and bone development. J Cell Sci 2009;122:716-26.
22. Kim JH, Kim K, Kim I, et al. Adaptor protein CrkII negatively regulates osteoblast differentiation and function through JNK phosphorylation. Exp Mol Med 2019;51:1-10.

23. Tao F, Jiang T, Tao H, et al. Primary cilia: Versatile regulator in cartilage development. Cell Prolif 2020;53:e12765.
24. Li M, Yin H, Yan Z, et al. The immune microenvironment in cartilage injury and repair. Acta Biomater 2022;140:23-42.
25. Huang Z, Wei H, Wang X, et al. Icariin promotes osteogenic differentiation of BMSCs by upregulating BMAL1 expression via BMP signaling. Mol Med Rep 2020;21:1590-6.
26. Wei Q, Wang B, Hu H, et al. Icaritin promotes the osteogenesis of bone marrow mesenchymal stem cells via the regulation of sclerostin expression. Int J Mol Med 2020;45:816-24.
27. Ma HP, Ma XN, Ge BF, et al. Icariin attenuates hypoxia-induced oxidative stress and apoptosis in osteoblasts and preserves their osteogenic differentiation potential in vitro. Cell Prolif 2014;47:527-39.
28. Li X, Xu Y, Li H, et al. Verification of pain-related neuromodulation mechanisms of icariin in knee osteoarthritis. Biomed Pharmacother 2021;144:112259.
29. Zhang Y, Shen L, Mao Z, et al. Icariin Enhances Bone Repair in Rabbits with Bone Infection during Post-infection Treatment and Prevents Inhibition of Osteoblasts by Vancomycin. Front Pharmacol 2017;8:784.
30. Shi W, Gao Y, Wang Y, et al. The flavonol glycoside icariin promotes bone formation in growing rats by activating the cAMP signaling pathway in primary cilia of osteoblasts. J Biol Chem 2017;292:20883-96.
31. Zhou L, Poon CC, Wong KY, et al. Icariin ameliorates estrogen-deficiency induced bone loss by enhancing IGF-I signaling via its crosstalk with non-genomic ERα signaling. Phytomedicine 2021;82:153413.
32. Tan Y, Tan L, Huang S, et al. Content Determination of Active Component in Huangqi Yinyanghuo Group and Its Effects on hTERT and Bcl-2 Protein in Osteosarcoma. J Anal Methods Chem 2014;2014:769350.
33. Ni T, Lin N, Huang X, et al. Icariin Ameliorates Diabetic Cardiomyopathy Through Apelin/Sirt3 Signalling to Improve Mitochondrial Dysfunction. Front Pharmacol 2020;11:256.
34. Huang H, Zhang ZF, Qin FW, et al. Icariin inhibits chondrocyte apoptosis and angiogenesis by regulating the TDP-43 signaling pathway. Mol Genet Genomic Med 2019;7:e00586.
35. Yuan B, Wu Z. MMP-2 silencing reduces the osteogenic transformation of fibroblasts by inhibiting the activation of the BMP/Smad pathway in ankylosing spondylitis. Oncol Lett 2018;15:3281-6.
36. Sulkowski MJ, Han TH, Ott C, et al. A Novel, Noncanonical BMP Pathway Modulates Synapse Maturation at the Drosophila Neuromuscular Junction. PLoS Genet 2016;12:e1005810.
37. Scarfì S. Use of bone morphogenetic proteins in mesenchymal stem cell stimulation of cartilage and bone repair. World J Stem Cells 2016;8:1-12.
38. Zhang XY, Li HN, Chen F, et al. Icariin regulates miR-23a-3p-mediated osteogenic differentiation of BMSCs via BMP-2/Smad5/Runx2 and WNT/β-catenin pathways in osteonecrosis of the femoral head. Saudi Pharm J 2021;29:1405-15.
39. García-García P, Ruiz M, Reyes R, et al. Smurf1 Silencing Using a LNA-ASOs/Lipid Nanoparticle System to Promote Bone Regeneration. Stem Cells Transl Med 2019;8:1306-17.
40. James AW, LaChaud G, Shen J, et al. A Review of the Clinical Side Effects of Bone Morphogenetic Protein-2. Tissue Eng Part B Rev 2016;22:284-97.
41. Draenert FG, Nonnenmacher AL, Kämmerer PW, et al. BMP-2 and bFGF release and in vitro effect on human osteoblasts after adsorption to bone grafts and biomaterials. Clin Oral Implants Res 2013;24:750-7.
42. Chen NF, Smith ZA, Stiner E, et al. Symptomatic ectopic bone formation after off-label use of recombinant human bone morphogenetic protein-2 in transforaminal lumbar interbody fusion. J Neurosurg Spine 2010;12:40-6.
43. Kawai M, Bessho K, Kaihara S, et al. Ectopic bone formation by human bone morphogenetic protein-2 gene transfer to skeletal muscle using transcutaneous electroporation. Hum Gene Ther 2003;14:1547-56.
44. Li XZ, Zhang SN. Herbal compounds for rheumatoid arthritis: Literatures review and cheminformatics prediction. Phytother Res 2020;34:51-66.

Cite this article as: Jiao F, Tang W, Wang J, Liu D, Zhang H, Tang D. Icariin promotes the repair of bone marrow mesenchymal stem cells in rabbit knee cartilage defects via the BMP/Smad pathway. Ann Transl Med 2022;10(12):691. doi: 10.21037/atm-22-2515

